ELSEVIER

Brain Research 891 (2001) 78–93

BRAIN RESEARCH

www.elsevier.com/locate/bres

Research report

In vivo Hebbian and basal forebrain stimulation treatment in morphologically identified auditory cortical cells

Scott J. Cruikshank, Norman M. Weinberger*

Center for the Neurobiology of Learning and Memory and Department of Neurobiology and Behavior, University of California, Irvine, CA 92717, USA

Accepted 31 October 2000

Abstract

The present study concerns the interactions of local pre/postsynaptic covariance and activity of the cortically-projecting cholinergic basal forebrain, in physiological plasticity of auditory cortex. Specifically, a tone that activated presynaptic inputs to a recorded auditory cortical neuron was repeatedly paired with a combination of two stimuli: (1) local juxtacellular current that excited the recorded cell and (2) basal forebrain stimulation which desynchronized the cortical EEG. In addition, the recorded neurons were filled with biocytin for morphological examination. The hypothesis tested was that the combined treatment would cause increased potentiation of responses to the paired tone, relative to similar conditioning treatments involving either postsynaptic excitation alone or basal forebrain stimulation alone. In contrast, there was no net increase in plasticity and indeed the combined treatment appears to have decreased plasticity below that previously found for either treatment alone. Several alternate interpretations of these results are discussed.

Theme: Neural basis of behaviour

Topic: Neural plasticity

Keywords: Neocortex; Cortex; Biocytin; Nucleus basalis; EEG; Hebb; Covariance

1. Introduction

Recent experiments on physiological plasticity of adult sensory cortex have found support for a modified form of the Hebbian hypothesis, which is sometimes called the 'covariance hypothesis.' It posits that the strength of synapses can be affected by relative levels of pre- vs. postsynaptic activity (i.e. pre/postsynaptic covariance). Specifically it predicts that pairing presynaptic input with increased postsynaptic activity should strengthen paired synapses, while pairing presynaptic input with decreased postsynaptic activity should weaken paired synapses [1,22,23,31,35,60,62].

Cells in the adult auditory cortex appear to follow the predictions of the covariance hypothesis, but the degree to which this occurs can be strongly affected by certain conditions [2,4,18,24]. One condition reported to be critical is 'arousal state.' For example, in urethane-anesthetized guinea-pigs, Hebbian/covariance pairing treatments result in greatest plasticity when those pairings are conducted in auditory cortices exhibiting nonsynchronized, low-voltage fast-wave EEG activity [24]. Facilitation of Hebbian plasticity in a way that is reminiscent of the EEG-related effects observed in the anesthetized guinea-pig, has also been observed in the auditory cortices of unanesthetized primates [2,4]. Together, these results suggest that activated/aroused cortical or behavioral states facilitate induction of covariance plasticity. However, the variables critical to plasticity that are associated with such arousal have yet to be defined.

Insight might be obtained by examining the role of the

*Corresponding author. Tel.: +1-949-824-5512; fax: +1-949-824-8481.

E-mail address: nmweinbe@uci.edu (N.M. Weinberger).

0006-8993/01/$ – see front matter
PII: S0006-8993(00)03197-8

cortically-projecting basal forebrain cholinergic system. Cells of the basal forebrain (BasF) provide the majority of acetylcholine (ACh) to the neocortex (reviewed in Mesulam [49]) [59]. Many findings indicate that ACh is involved in EEG arousal [53](reviewed in Steriade [63]), including the observations that BasF stimulation causes increases in cortical ACh and EEG nonsynchrony [10,19,28,39,44,50,51]. ACh is thought to mediate at least some of the cellular effects produced during EEG arousal [63]. One effect of ACh on cortical neurons is increased excitability, resulting from muscarinically-mediated decreases in potassium conductances [48,61]. Thus, facilitation of Hebbian/covariance plasticity during EEG nonsynchrony (above), may be mediated by ACh, which could increase postsynaptic excitability during covariance pairings. This might enhance postsynaptic response to afferent inputs beyond that already imposed by the experimenter (above), facilitating Hebbian synaptic potentiation.

Auditory cortical responses to sensory input can be increased by stimulating the BasF immediately preceding sensory input and these effects are blocked by atropine, implicating muscarinic cholinergic mechanisms [28,50,51]. Also, pairing sensory inputs with BasF stimulation, without direct postsynaptic manipulation, can result in long-term plastic increases in response to the paired inputs [10,15,25,28,34,41]. This type of plasticity, which will be referred to as 'BasF pairing plasticity,' has been reported for ACx and other neocortical regions [26,66].

The long-term enhancement produced by pairing sensory input with BasF stimulation may be induced via Hebbian mechanisms [3]. Specifically, BasF stimuli could provide cholinergic excitation of cortical neurons at the time of incoming sensory evoked transmission. According to the Hebbian hypothesis, this could cause the widely reported long-term enhancement in response to the paired sensory inputs. Although this proposed mechanism has seldom been addressed experimentally, it is not a novel idea. In fact, 'Hebbian explanations' have previously been proposed as likely mechanisms by which BasF pairing plasticity is induced [26,40,66]. Furthermore, this Hebbian explanation for the BasF pairing plasticity is only subtly different from the proposed cholinergic explanation for the state-related facilitation of covariance plasticity discussed earlier. The two hypothetical explanations/mechanisms actually share the same underlying events, and differ only in which variables are controlled by the experimenter.

The present study is an attempt to directly address these issues. Specifically, we asked whether or not combining Hebbian and BasF pairings in ACx, within the same experimental treatment, would produce greater plasticity than that expected for either treatment on its own. Furthermore, efforts were made to label the recorded neurons with biocytin to determine if cells exhibiting physiological plasticity have any predisposing morphological characteristics.

2. Materials and methods

2.1. Summary of the experimental design

For each auditory cortical cell recorded (referred to as postsynaptic cells), two acoustic stimuli of differing frequency were presented to activate two different populations of presynaptic afferents. One of these stimuli served as a paired input (CS+) while the other served as a neutral control (CSn). Following determination of baseline postsynaptic responses to both stimuli, a pairing treatment was imposed. During this treatment, the CS+ was repeatedly paired with a combination of excitatory postsynaptic current (juxtacellular, see below) and BasF stimulation. The juxtacellular current was applied in order to increase postsynaptic excitability and discharge, thereby increasing covariance between activity of the postsynaptic cell and its afferents that were activated by the CS+ tone. The BasF stimuli were applied to activate neurons of the BasF that project to the ACx and cause cortical EEG desynchrony as well as release of cortical ACh during the pairings. After the treatment, the relative effects on functional synaptic strength for the paired CS+ and the control CSn were examined.

2.2. Subjects and initial surgery

Subjects were adult male Sprague–Dawley rats ($n=28$; 252–430 g). Bipolar stimulating electrodes were implanted into the BasF region during an initial sterile surgery using coordinates previously found by Bakin and Weinberger [10] to be successful for eliciting EEG desynchrony in ACx (below). Animals were injected with atropine (0.08 mg/kg, i.p.) and diazepam (8 mg/kg, i.p.) followed 15 min later by Nembutal (20 mg/kg, i.p.). Supplementary doses of Nembutal were given as needed to maintain adequate levels of anesthesia throughout the surgery. Animals were placed on a heating pad, and secured to the stereotaxic apparatus with blunt ear bars. After initial incision and resection of scalp and periosteum, stainless steel screws were threaded into the calvaria to anchor an acrylic pedestal containing threaded metal tubes. These were bolted to a frame attached to the stereotaxic apparatus to secure the skull without ear bars in both the initial surgery and during the later experiment (below). Burr holes were made in the skull dorsal to the BasF (from bregma: 2.0 mm posterior, 2.7 mm lateral). The dura mater was resected and bipolar stimulating electrodes (two twisted stainless steel wires, 100 μm diameter) were lowered 7.0 mm below the surface of the brain. The electrodes were fixed to the pedestal with dental cement, the wound closed, and local antibiotics administered to the skin (Panalog, neomycin sulfate). Following recovery in an incubator, the animals were returned to their home cages until the day of the experiment (8.3±7.1 S.D. days following implant).

2.3. Preliminary procedures on the experimental day

Rats were anesthetized with Urethane (ethyl carbamate, 1.45 gm/kg, i.p.) and supplemented as needed to maintain areflexia. An opening was made in the skull over temporal cortex, and ACx was located by position, vascular landmarks, and click-evoked field potentials. Small holes were cut in the dura to allow insertion of a juxtacellular recording/stimulating micropipette into ACx. Core body temperature was maintained at 37°C with a heating pad. Auditory cortical EEG was monitored continuously from either the juxtacellular recording electrode (below) or from a tungsten microwire on the cortical surface (bandpass 1–100 Hz, single-ended recordings, animal grounded via skin flap). The maximum lateral distance between the surface and juxtacellular electrodes was about 3 mm (usually they were within 1 mm of each other). At the beginning of the recording session, a test was administered to determine the threshold current level at which BasF stimulation could desynchronize the EEG of the ipsilateral ACx (0.1 ms biphasic pulses, 200 Hz, 200 ms train, 100–500 μA). Later, during the pairing treatment (below), BasF stimuli were delivered at an intensity sufficient to produce continuous desynchrony, up to a maximum of 500 μA (mean=64±25% above threshold).

2.4. Juxtacellular recording and stimulation

The juxtacellular microelectrode (glass micro-pipette, tip diameter 0.5–1.5 μm) was filled with a solution consisting of 140 mM K-gluconate, 1.0 mM $MgCl_2$, 1.0 mM $CaCl_2$, 10.0 mM HEPES buffer, and 1.6 mM EGTA. DC resistances were 3–8 MOhms (mean=5.7±0.3 S.E.M.). The solution also contained a 2% concentration of biocytin so that the recorded cells could be labeled and subsequently identified (below).

At the beginning of an experiment, the juxtacellular electrode was advanced perpendicular to the cortical surface by a stepping micro-drive. At a depth of 200–400 μm, the penetration was temporarily halted and the cortex was covered with warmed agar (4% in saline) to prevent pulsation. In most cases, cisternal puncture and tracheal cannulation were also used to minimize cortical movement. After allowing the electrode to settle for 10 min, the penetration was resumed, and the search for a single cortical neuron commenced (approximately 1 μm/s for 5–10 s, followed by 5–10 s pauses before advancing further). During this search, acoustic stimuli were presented while physiological activity (DC — 6 kHz, amplified ×100) and electrode resistance were monitored.

Upon detection of small extracellular action potentials (<1 mV), the electrode was carefully advanced further until a juxtacellular recording configuration could be achieved. This was operationally defined as a recording with very large action potentials (>2 mV) having a positive polarity initial phase and an increase in electrode resistance (>20%) upon achieving the configuration. These operational features were taken as an indication that the tip of the microelectrode was situated very close to the recorded soma, probably directly contacting the membrane [5,22,24,38]. In this configuration, low levels of current (=20 nA, 100 ms, tip positive) applied through the micropipette could effectively elicit action potentials, as previously reported [5,14,16,17,24,32,57,64,68]. A bridge circuit allowed uninterrupted recording during current pulses.

2.5. Characterization of responses to tones and juxtacellular current

The protocol following cellular isolation is summarized in Fig. 1. First the receptive field (RF) of the neuron was characterized. Tones were delivered to the ear contralateral to the recording locus via a calibrated acoustic delivery system (100 ms pure tones, 0.1–30 kHz, 0–90 dB, rise/fall times 5 ms, 1 tone/s), using a small speaker fixed in place at the opening of the external auditory meatus (near field, [65]). Threshold tuning curve, best frequency (BF), and evoked spike rates for the different tone frequencies within the RF were determined. Two tones were chosen from the RF for subsequent experimental phases. One of these tones was defined as the CS+, and was paired with juxtacellular and BasF stimuli during the upcoming treatment. The other tone was defined as the CS neutral (CSn) and served as an unpaired control.

The CS+ and CSn tones were different frequencies (one lower than the BF, the other higher than the BF, counterbalanced across cells) and were presented at the same intensity for a given cell. On average this intensity was 24 dB above the threshold of the cell: mean threshold (at the BF) was 35(±6 S.E.M.) dB and mean intensity used for the CS tones was 59(±3 S.E.M.) dB. The mean frequency chosen as the CS+ was 0.5(±0.1) octaves from the BF, and the mean CSn was 0.4(±0.2) octaves from the BF. The average baseline response to the CS+ was slightly weaker, than the response to the CSn (11.6±1.4 vs. 13.9±1.7 spikes/s, respectively) but not significantly different (*t*-test, $P>0.05$). Comparison with the mean response to the BF tone (22.4±3.4 spikes/s, presented at the same intensity as the CS tones) revealed that the baseline responses to both the CS+ and CSn were moderate (55–64% of those elicited by the BF), allowing for possible increases and decreases that might occur as the result of the treatment.

After choosing the CS tones, the response to positive juxtacellular current was characterized by determining threshold, spike rate and latency. A value that was above the threshold for eliciting spikes, but was not so high as to de-stabilize the recording, was selected for subsequent pairing (mean threshold=8.8±1.1 nA, mean pairing intensity=12.6±1.5 nA).

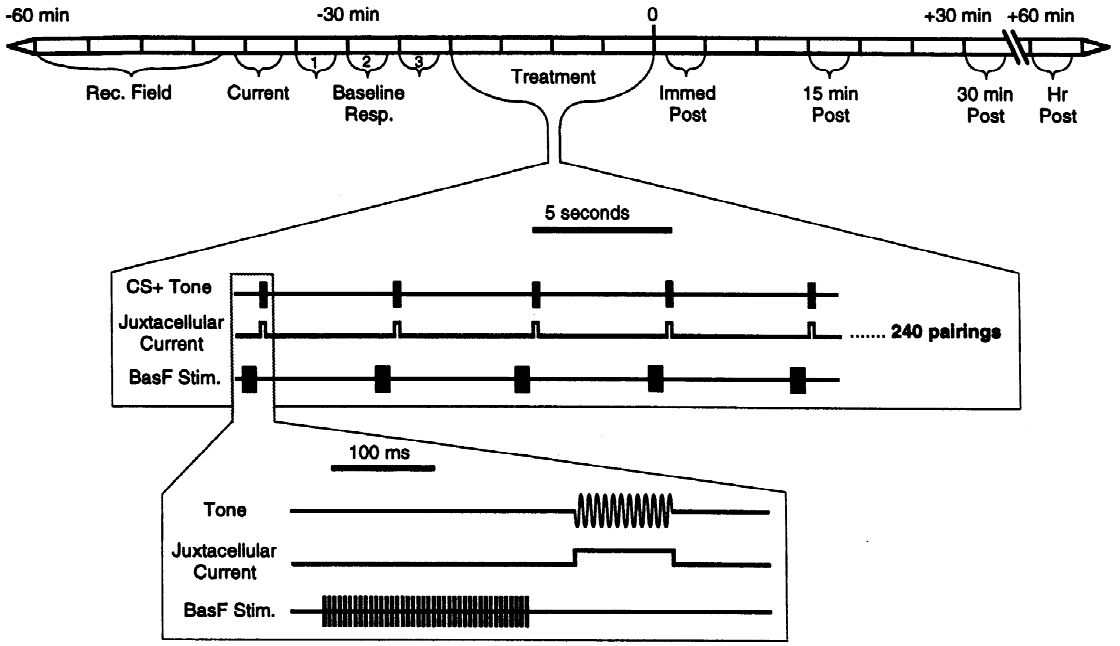

Fig. 1. Experiment protocol. The temporal position of each experimental period is shown on the timeline (top). The treatment is depicted in the middle. Timing of stimuli for a single pairing trial is shown on the bottom.

2.6. Baseline, treatment, and post-treatment procedures

The response characterizations were followed by a 15 min baseline period, during which the stability of responses to 60 presentations of the CS+ and CSn tones were measured (separated into three blocks, with 20 interleaved presentations of each tone per block, 0.2 Hz stimulus rate). Next, a treatment was administered in which the CS+ tone was repeatedly paired with simultaneous juxtacellular current (240 pairings at 0.2 Hz; tone and juxtacellular current durations were 100 ms; Fig. 1). In addition, each tone/current pairing was preceded by a 200 ms train of BasF stimulation, that was adjusted to produce EEG desynchrony in the ACx (0.1 ms biphasic current pulses, 100 Hz, 100–500 μA, onset of train began 250 ms prior to the tone). Immediately following the treatment and at 15 min intervals for up to an hour, the responses to the tones alone were re-determined (20 trials each, CS+ and CSn interleaved as during the baseline, without any current).

2.7. Data analysis

The spike rate responses evoked by each presentation of the CS+ and CSn were collected during the baseline, treatment, and post-treatment periods. These spike rates were averaged over the 100 ms of tone duration (for all cells during all experimental periods) in order to capture the majority of evoked spikes, while avoiding periods of inhibition that often followed offset of the tone. The relative response to the CS+ vs. the CSn was calculated for each baseline and post trial (a trial=one sequential presentation of the CS+ and CSn) as follows:

$$\text{CS+/CSn Index} = \frac{(\text{spike rate to CS+})}{(\text{spike rate to CS+}) + (\text{spike rate to CSn})}$$

The potential values of the CS+/CSn Index range from 0.0 to 1.0. A value close to 1.0 indicates a strong preference for the CS+, a value close to 0.0 indicates a strong preference for the CSn, and a value close to 0.5 indicates about equal responses for the CS+ and CSn.

Analysis of variance (ANOVA) was used to examine the stability of the Index scores across the three baseline blocks. Only those neurons that were stable (indicated by $P>0.05$), were used in subsequent analyses. After determining that the three baseline blocks were not significantly different from one-another, they were collapsed into a single block for comparison with the treatment and post-treatment periods. Unpaired *t*-tests were used to examine differences between the baseline period and other periods (significant difference, $P<0.05$).

2.8. Histological localization of the BasF electrodes

At the end of a recording session, the BasF stimulating electrode positions were marked by passing direct current (5–10 μA, 10 s) between the two poles of the stimulating electrode. Animals were then euthanized with an overdose of urethane and intracardially perfused with phosphate buffered saline (9 g NaCl per liter of 0.02 M phosphate buffer) followed by 4% paraformaldehyde fixative (40 g

paraformaldehyde per liter of 0.1 M phosphate buffer). The brains were removed from the skull and stored in 4% paraformaldehyde for 1–3 days, then in a solution of 20% sucrose (w/v) in 4% paraformaldehyde for 1–3 days (4°C for both solutions). Brains were cut on a freezing microtome in the coronal plane (40–100 μm thickness). Sections from the rostral regions, which contained the BasF, were stained with Cresyl Violet. Locations of lesion marks were compared with boundaries derived from the rat brain atlas of Paxinos and Watson [55] to determine BasF electrode locations. Sections from the caudal regions, which contained the ACx, were stored in phosphate buffer (PB) for visualization of the recorded cells as described next.

2.9. Juxtacellular labeling and histology

The recorded cells were labeled with biocytin using the method of Pinault [57,58]. Cells were isolated in a juxtacellular configuration with micropipettes filled with 2% biocytin solution as described above. Positive current stimuli were delivered through the micropipette during the current characterization phase and during the pairing treatment as described above. These stimuli appear to eject Biocytin from the pipette into the neuron [58]. Following a survival period (between 45 min and 8 h; mean = 230 ± 30 min) the brain was fixed and sectioned as indicated above.

Standard visualization methods, modified from Horikawa and Armstrong [36], were applied. Sections were incubated for 10 min in a 0.2% concentration of H_2O_2 in phosphate buffer (PB), followed by PB rinses, then incubated overnight in avidin–biotin–peroxidase solution at 4°C, on a rotator (Standard ABC kit, Vector Labs, 0.3% Triton X-100 in PB). The next day sections were rinsed in PB, pre-incubated in 0.01% DAB solution for 10 min, then reacted by adding 60 μl of 30% H_2O_2 to each 100 ml of DAB solution. After 20 min the sections were rinsed with PB, mounted on slides, air-dried, then lightly counterstained with Cresyl Violet to facilitate the demarcation of laminar boundaries. Finally sections were dehydrated, cleared and coverslipped for microscopic examination.

The representations of the cells presented below are either camera lucida reconstructions, or computer images captured from a laser confocal microscope. For clarity, blood cell artifacts were attenuated, and contrast enhanced, using Adobe Photoshop.

2.10. Habituation control

Habituation control experiments were conducted for an additional nine cells ($n = 6$ animals) to test whether or not repeated presentation of one tone frequency would cause a specific decrease in ACx responses to that frequency, relative to a control frequency that was not presented during the treatment. The protocol consisted of RF and Baseline periods identical to the other experiments (above). Next was a Treatment phase that simply consisted of 240 repeated presentations of one tone frequency, at 0.2 Hz. Finally Post-Treatment periods identical to the other experiments were conducted. No current stimuli were delivered at any time. Furthermore, the recording pipette contained no biocytin. For analysis, the repeated tone (CSr) substituted for the CS+, and replaced it in the CS+/CSn Index.

3. Results

3.1. Juxtacellular labeling of physiologically identified cells with biocytin

From an initial total of 201 acoustically responsive units from 28 animals, 53 were successfully isolated in a juxtacellular configuration and characterized quantitatively for their acoustic receptive fields and current evoked responses. Of these, 15 cells (from 12 rats) were 'held' throughout the baseline, treatment, and post-treatment periods. Finally, 10 of these 15 cells were successfully labeled with Biocytin. For all labeled cells, at least the soma and major proximal dendrites were stained. Dendritic spines were often visible. Axonal labeling was never complete, although the initial portions of the axons could sometimes be seen. The 10 recovered neurons included eight pyramidal cells, identified by the presence of an obvious apical dendrite. These were distributed as follows: Layer III = 1, Layer IV = 5, Layer V = 1, Layer VI = 1. The two remaining neurons had no obvious apical dendrites, and were classified as non-pyramidal cells. Both of the non-pyramidal cells were located in Layer IV. One had high spine density while the other had no obvious spines.

Fig. 2 presents confocal microscopic images of two recovered cells and their corresponding acoustically driven responses. Fig. 2A shows a Layer IV non-pyramidal cell. It has a high spine density and is multipolar in form, with many dendritic branches emanating in all directions from the soma. Based on morphology and position, this cell appears to be a layer IV spiny stellate cell [56]. In support of this, the cell displayed robust, short latency responses to tones (approximately 20 ms; Fig. 2B) as might be expected of a primary recipient of thalamocortical input [56]. Further physiological characterization of this cell revealed a reasonably low acoustic threshold (20–25 dB), and narrow tuning: ≤0.25 octave response range at 20 dB above threshold (Fig. 2B). For comparison, Fig. 2C shows a pyramidal cell from deep layer 6. It has an ovoid soma located <100 μm from the subcortical white matter and an apical dendrite that terminates in layer IV with a bouquet of branches. In contrast to the layer IV cell discussed above, this infragranular pyramidal cell displayed longer latency responses to acoustic stimuli (>40 ms; Fig. 2D) and broad frequency tuning: ≥1.5 octaves range at 20 dB

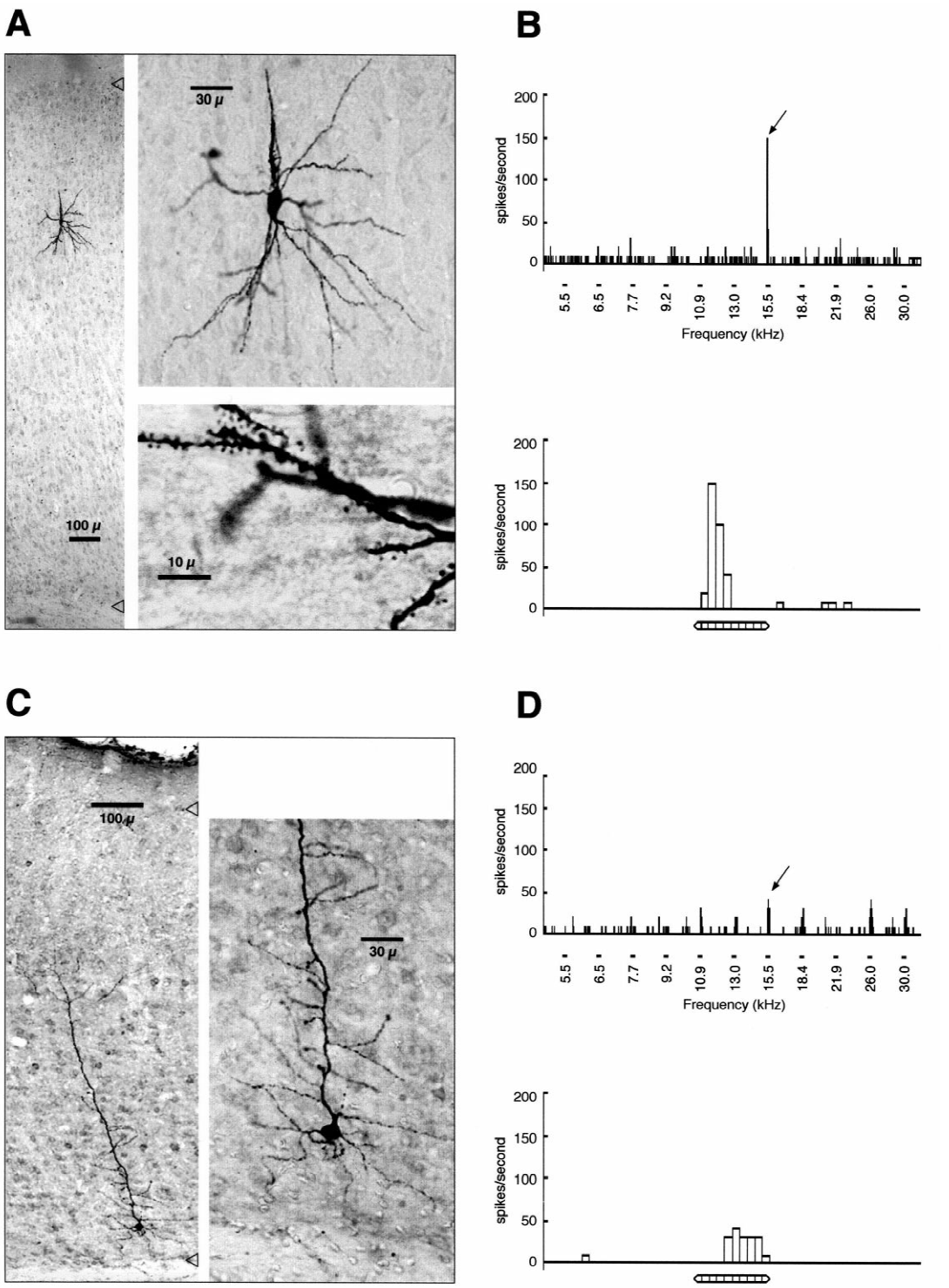

Fig. 2. Morphology and acoustic responses of two auditory cortical cells. (A) Morphology of a of spiny non-pyramidal cell (≠BH2406). Far left is low magnification image showing position of soma in layer IV. Open arrows positioned at layer I/II border and bottom of layer VI. Upper right shows medium power image of the soma and dendrites. Note the lack of apical dendrite. Bottom right is magnified view of the dendrites that project ventrally from the soma (they are rotated 90 degrees in the display). Note the high spine density. (B) Acoustic response of the cell visualized in 'A'. Top shows the peristimulus time histograms and raster plots for a range of tone frequencies presented at 45 dB. Note that there is a significant response at only one of the frequencies (15.5 kHz). Bottom shows the response latency and pattern for the 15.5 kHz tone. The bin width is 10 ms. The bin with the largest number of spikes begins 20 ms following the stimulus onset, and the response ends within 50 ms of stimulus onset. (C, D) Morphology and acoustic responses of a deep layer VI pyramidal cell (≠BH3212). The cell has an obvious apical dendrite that extends to approximately layer IV, typical of layer VI cells (C). Tuning is broad (D, top), responses are relatively weak, and latencies are long (=40 ms at the best frequency; D, bottom). Tissue is counterstained with Cresyl Violet in A and C.

above threshold (Fig. 2D). Possible relationships between morphological characteristics and plasticity will be discussed below.

3.2. Effects of basal forebrain stimuli during the pairing treatment

BasF stimulation during the pairing treatments generally produced desynchronization of the EEG (below). An example is shown in Fig. 3. EEG records and associated frequency power spectra are plotted for periods before, during, and after the treatment. [Note the sudden shift from large slow waves during the baseline to low amplitude faster waves during the treatment (which included BasF stimulation: see Materials and methods)]. For this experiment there was clear EEG desynchrony on nearly every trial. For the initial trials, there was some recovery between stimuli. However, by the middle of the treatment, the desynchrony was continuous, lasting the full 5 s between trials. Finally, following termination of the treatment, there was a gradual and complete recovery of synchronous activity.

Of the 15 experiments that were completed, four were similar to the example shown in Fig. 3; i.e. there was desynchronous EEG on greater than 90% of the treatment trials. These experiments were classified as 'desynchronized.' For seven experiments, the BasF stimulus induced desynchrony for 50–90% of the treatment trials. These were classified as 'mixed.' Finally, for four experiments, the BasF stimulus was ineffective, having no effect on the cortical EEG; they were classified as 'synchronized.' Figs. 4A, B shows examples of the three categories of EEG effects [24]. Fig. 4C plots the stimulation electrode placements as a function of EEG state during the treatment.

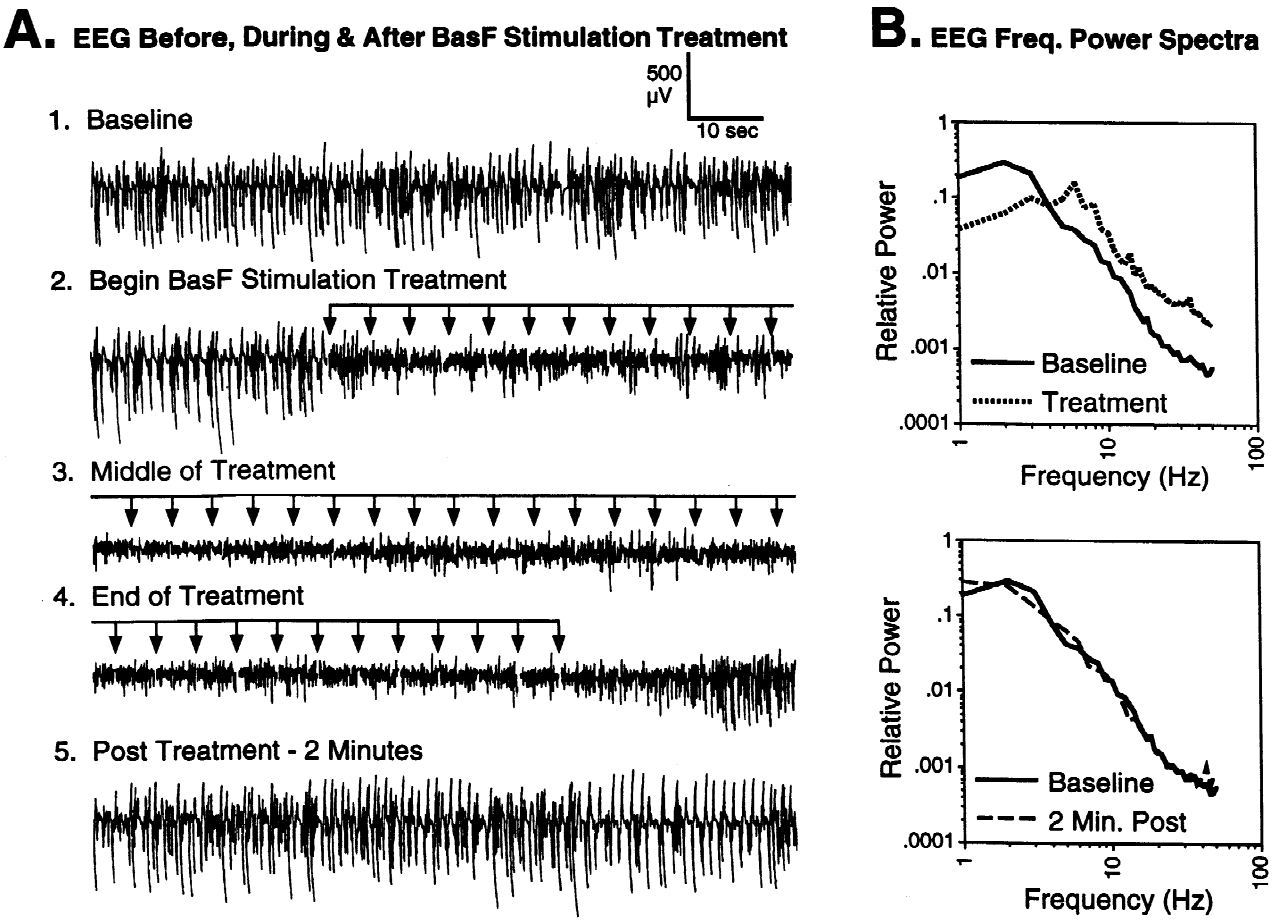

Fig. 3. Example of BasF stimulus that desynchronized the EEG during treatment. (A) EEG activity obtained from the ACx before during and after BasF stimulation (recorded at a depth of 683 μm and bandpass filtered 1–75 Hz). During the treatment, trains of BasF stimuli are delivered every 5 s (indicated by arrows). Notice the time-locked decrease in large amplitude slow waves beginning immediately after BasF stimulation (2). By the 'middle of treatment' the EEG remains completely desynchronized between stimulus trains (3). After the 'end of treatment' the EEG gradually recovers toward pre-treatment levels (4). Within 2 min of terminating stimulation, the large slow wave activity has fully recovered (5). (B) The frequency power spectra are obtained from the 3 s periods centered between the BasF stimuli. Note the robust decreases in low frequencies and increases in high frequencies during the BasF stimulation treatment, relative to baseline (B, top). The spectrum recovers 2 min after the treatment (low frequencies are even more dominant in the post-treatment phase; B, bottom), indicating that it was the BasF stimulation and not spontaneous drifting of state, that produced the changes.

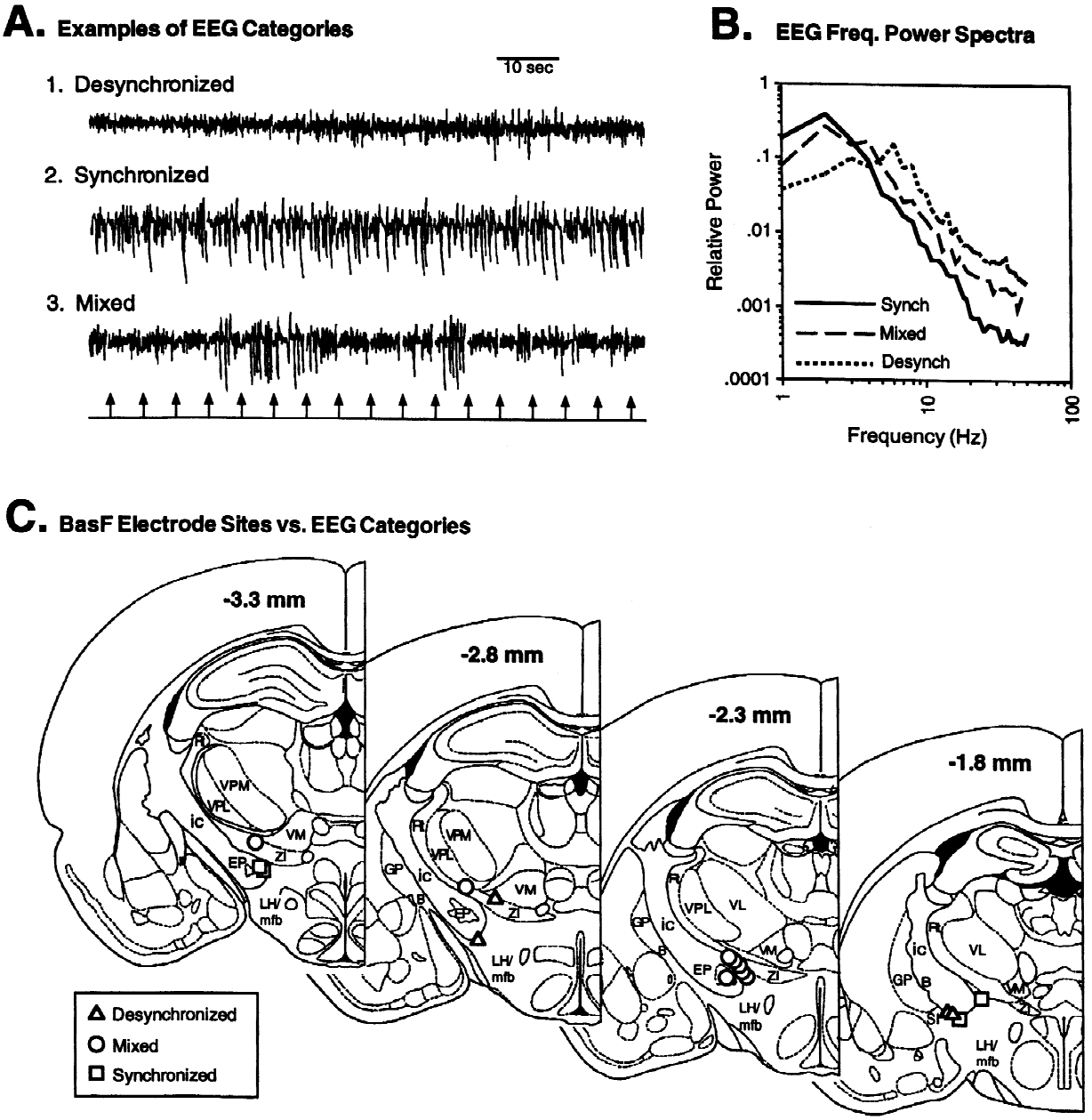

Fig. 4. Categories of EEG responses and the position of electrodes for BasF stimuli. (A) Examples of each category of EEG responses to BasF stimulation (stimuli indicated by arrows; polygraph recordings are bandpass filtered @ 1–75 Hz). Records taken from middle of treatment phases. Each example comes from the ACx of a different rat. See text for explanation of classifications. (B) Frequency power spectra associated with each of the experiments illustrated in 'A'. Again, power spectra were calculated from 3 s periods centered between the BasF stimuli. Note the progressive decreases in slow waves and increases in fast waves, as one examines first the synchronized, then the mixed, and finally the desynchronized power spectra. (C) BasF stimulating electrode loci, determined histologically, and plotted according to EEG category during the treatment. Numbers on sections represent distance from bregma (Adapted from [52]). Abbreviations: B, cells of the basal nucleus of Meynert; EP, entopeduncular nucleus; GP, globus pallidus; ic, internal capsule; LH/mfb, lateral hypothalamus/medial forebrain bundle; Rt, reticular thalamic nucleus; SI, substantia innominata; VM, ventromedial thalamic nucleus; VPL, ventrolateral thalamic nucleus; VPM, ventroposterior thalamic nucleus, medial division; ZI, zona incerta.

Loci included a variety of nuclei and tracts in and around the BasF region, between 1.8 and 3.3 mm posterior to bregma. There was no clear relationship between anatomical position and effect on the EEG within the regions stimulated here.

3.3. An increase in pre/postsynaptic covariance was imposed during the treatment

During the treatment, application of the positive juxtacellular current significantly increased the responses to

the CS+. This was consistent for both the group data, where the mean response imposed during the treatment was nearly three-fold above baseline (Fig. 5), and in the individual data, where each of the 15 cells tested exhibited significant increases ($P<0.05$, *t*-test, treatment vs. baseline). It has previously been shown that the excitation produced by juxtacellular current using these stimulation parameters is highly localized to the postsynaptic cell [24] and can best be accounted for by direct current injection into the postsynaptic cell [22]. Thus, these imposed postsynaptic response increases indicate that the treatment effectively increased the covariance between the postsynaptic cells and the presynaptic afferents activated by the CS+ tones [23,24].

3.4. No significant post-treatment plasticity was observed across the population

Despite the effective treatment (above), there was no significant group change in the CS+/CSn Index immediately after the treatment ($P=0.9$, Immed. Post vs. Baseline), nor did changes emerge at the 15- or 30-min post-treatment measurement periods (Fig. 6; Ps>0.2). This stands in stark contrast to a previous study of auditory cortex [24], in which significant mean increases were induced immediately after a Hebbian treatment, and lasted for at least 15 min ($P<0.03$). The previous study did not include BasF stimulation. This suggests that the addition of the BasF stimuli in the present study did not augment the Hebbian plasticity as predicted, but instead may have attenuated plasticity (discussed below).

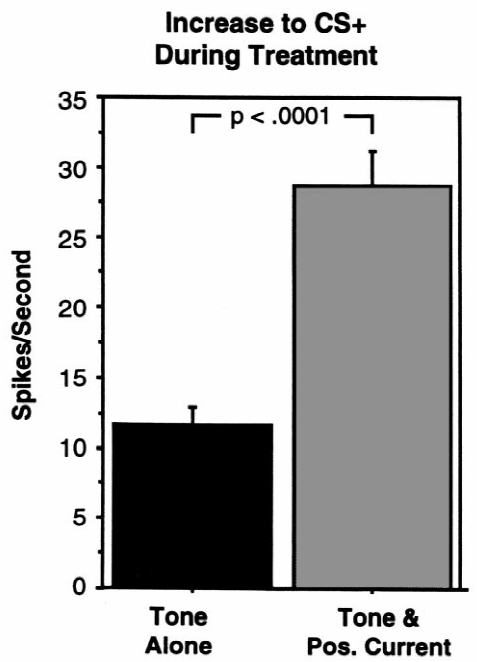

Fig. 5. Increases in responses imposed during covariance treatment. Mean group response ($n=15$) to the CS+ tones alone (baseline period, black bar) are compared with the group response to same tones in the presence of positive postsynaptic current (treatment period, grey bar). Probability shown is from paired *t*-test. Note the highly significant increase in response to the CS+ produced by the addition of positive current. This indicates that the addition of positive current was effective in increasing 'covariance' during the treatment. See text.

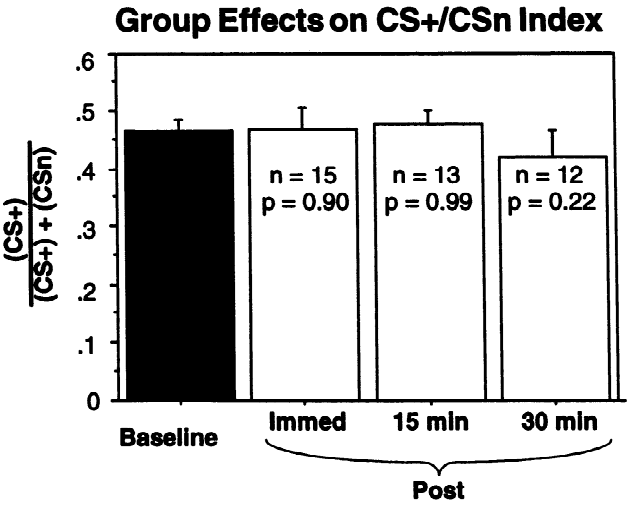

Fig. 6. Group effects for the CS+/CSn Index. The histograms compare the mean group CS+ vs. CS− index values for the baseline and each of the post-treatment periods. Measurement periods are labeled along the bottom. Number of cells for each period shown in the corresponding histogram. Probabilities are results of paired *t*-tests (posts vs. baseline, within-cell). Notice that there is no significant change relative to baseline for any of the post-treatment measures.

Analysis of the post-treatment results on an individual cell-by-cell basis confirm and extend the group results. Only one of the 15 neurons (6.7%) showed the predicted relative increase in the CS+ vs. CSn Index (Fig. 7A; $P<0.05$, Post vs. Baseline). Examination of the peristimulus time histograms for this 'plastic' cell reveals that the differential change was caused exclusively by an increase in the CS+ response; the response to the CSn did not change significantly (Fig. 7B). A second cell changed significantly in the non-predicted direction (i.e. relative CS+ decrease; $P<0.05$, not shown). The relative responses for both neurons returned to baseline levels within 15 min. Thus, as was the case for the group results, the individual cell data showed very little post-treatment plasticity. Furthermore, the two changes that did occur were in offsetting directions. Also in agreement with the group results, the individual cell data contrast with the previous Hebbian study from our laboratory, in which 7/22 (32%) cells exhibited significant relative increases immediately after a Hebbian treatment, while no cells showed decreases. Furthermore, six of those 'plastic' cells from the previous study maintained the changes for at least 15 min ($P<0.05$, [24]). Given the surprising finding that the treatment in the present study, which included the addition of BasF stimulation, induced less (rather than more) plasticity than the previous Hebbian treatment alone [24], we next focused our analysis and experiments on

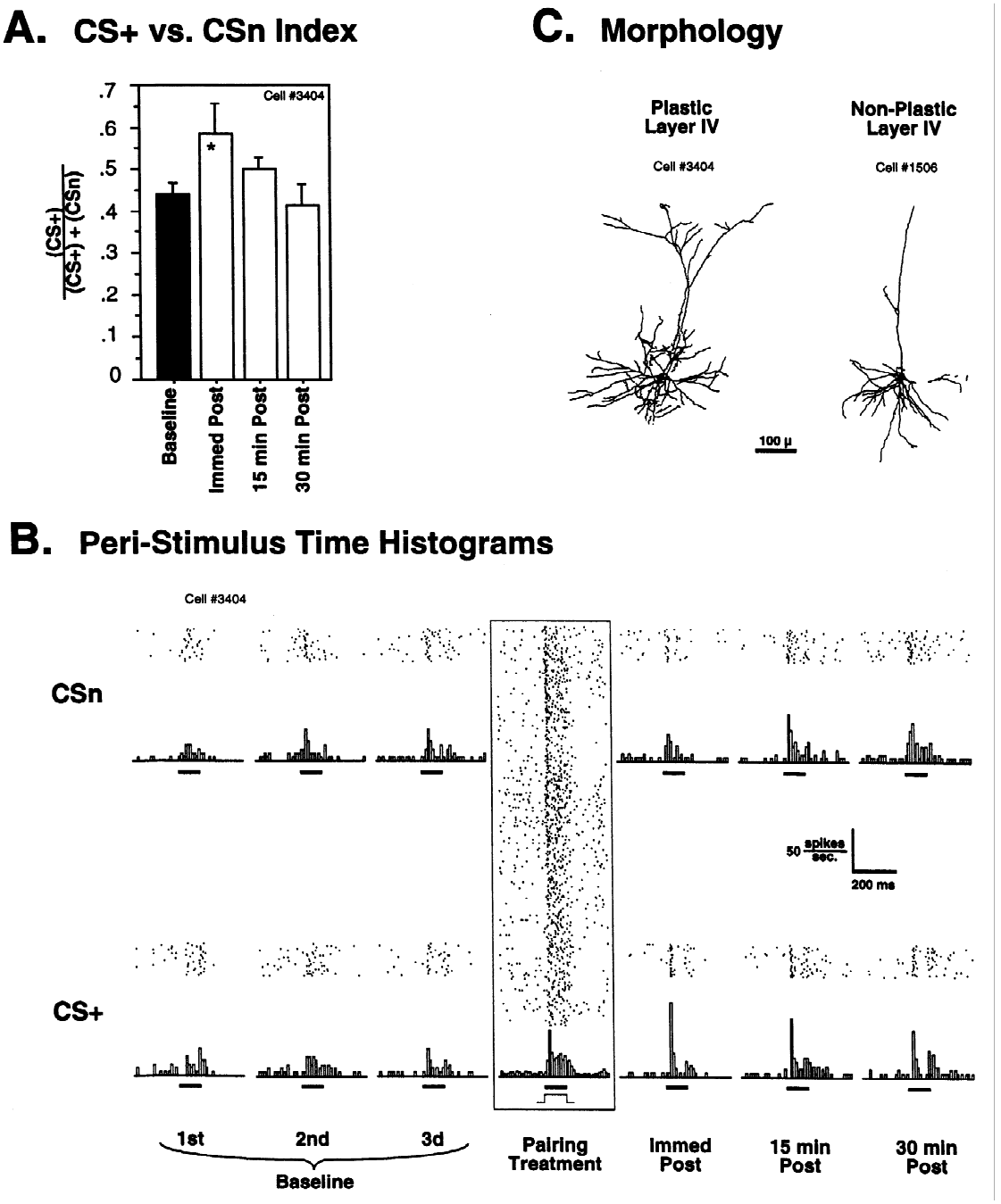

Fig. 7. Example increase in post-treatment response to CS+, and morphology. (A) Evolution of the Index values for the cell that underwent the significant increase. Measurement periods labeled along bottom. Note that the increase relative to baseline only remained significant for the first post-treatment measurement (asterisk indicates $P<0.05$). (B) Peri-stimulus time histograms (PSTs) and associated raster plots for the cell described in part 'A' of this figure. Separate responses to the CSn (top row) and the CS+ (bottom row) are shown. Bins are 10 ms. Response magnitudes in spikes/s (see calibration). Each dot in a raster represents a spike. Successive trials for a given period are stacked in rows upon one-another. The treatment period has more rows because it represent responses to 240 trials rather than 20 trials. The baseline CS+ response was modest, and the CSn response was slightly stronger, resulting in a baseline Index value of 0.44 ± 0.03. During the treatment, a significant increase in CS+ response was imposed ($P<0.0001$). Immediately after the treatment there was a significant increase in CS+ response compared to baseline ($P<0.02$), and a non-significant decrease to the CSn ($P=0.21$), resulting in a significant increase in the Index (Post $=0.59\pm0.07$, $P<0.04$). Note that along with the increase in mean rate, the response pattern also changed; after the treatment the CS+ elicited a robust 'on' type response. At 15 min, the CS+ response remained elevated, but the CSn response had increased as well, such that the Index value had fallen to non-significant levels ($P=0.30$). (C) The drawing on the left ('Plastic, Layer IV') shows the soma and dendrites of the cell exhibiting the significant increase following treatment, described in parts 'A' and 'B' of this figure. Note the large amount of branching off the distal portions of the apical dendrite (i.e. in the upper layers). The drawing on the right ('Non-Plastic, Layer IV') shows a layer IV cell that failed to display physiological plasticity. Note that the apical dendrite has only one small offshoot, with no branching in the distal upper layer region. Also see text.

possible explanations for the lack of strong plasticity in the present study.

3.5. Morphological observations: plastic vs. non-plastic cells

Both the number of morphologically recovered cells and the degree of physiological plasticity were quite limited. However, there are also very little data available on the relationship between morphology and plasticity in the neocortical literature. With this in mind, we attempted to extract whatever potentially useful information we could from our sample. The cell that exhibited the significant increase in the CS+/CSn Index is illustrated in Fig. 7C. It was determined to be a pyramidal cell, located in layer IV. Based on the simple criteria of (a) pyramidal vs. non-pyramidal cell type and (b) layer, the 'plastic' cell did not distinguish itself from several non-plastic cells; recall that there were six other cells recovered in Layer IV that completed the experiment (e.g., see Fig. 2A), including four pyramidal cells. None of these exhibited significant plasticity.

However, examination of gross dendritic morphology did reveal one obvious distinguishing feature of the 'plastic cell': the spread of the dendritic branching in the upper layers. The apical dendritic arbor of the plastic cell was broad, having a medial/lateral spread of approximately 450 μm (Fig. 7C; 'Plastic, Layer IV'). In contrast, the upper layer branching was quite sparse for the other layer IV pyramidal cells. The most extreme case, also shown in Fig. 7C ('Non-Plastic, Layer IV'), has no labeled branches in the upper layers whatsoever. In fact, the largest spread of apical dendritic branching for any of the non-plastic Layer IV cells was approximately 150 μm (not shown). Thus, the amount of upper layer branching seems to distinguish the plastic Layer IV pyramidal cell from the non-plastic Layer IV pyramidal cells. It remains to be determined whether or not such branching is important for plasticity.

The cell displaying the significant relative decrease in CS+ response was not recovered histologically. Based on microdrive measurements during the recording (923 μm from the pial surface), it was estimated that this cell was located in Layer V.

3.6. Effectiveness of BasF stimuli on cortical state vs. plasticity

As shown above, BasF stimulation produced non-synchronized EEGs for the majority of cases. However it may have had additional effects, particularly on plasticity, that were unexpected. To address this possibility, we first examined the magnitude of plasticity for the synchronous vs. nonsynchronous cell groups (nonsynchronous group composed of desynchronous and mixed as in [24]). This division is based on the premise that the BasF stimulus had less overall effect on the auditory cortices for the synchronous cases (which appeared unaffected on the independent measure of EEG) than for the nonsynchronous cases. Fig. 8 compares the plasticity for the two EEG categories and reveals that the four cells exhibiting the greatest relative increase in response to the CS+ (i.e. the greatest plasticity in the predicted direction) were actually the same four cells that composed the entire 'synchronous' EEG group. When considered as a separate unit, the cells of the synchronous group actually exhibited significant plasticity ($P<0.003$, paired t-test, post vs. baseline), whereas cells of the analogous nonsynchronous group did not ($P>0.05$). Observe that even the cell with the weakest increase for the synchronized group had a higher value than the strongest increase for the non-synchronized group (Fig. 8). Among the cells of the synchronized group was the one statistically significant positive effect previously illustrated in Fig. 7. Thus, contrary to expectations, BasF stimuli that were effective (as assessed by their effects on EEG), may have somehow 'prevented' the Hebbian treatment from inducing potentiation of CS+ responses.

One possible way in which BasF stimuli could negatively effect plasticity would be to reduce postsynaptic excitability during the treatment. This possibility was examined by comparing the pre-tone spike firing rates for

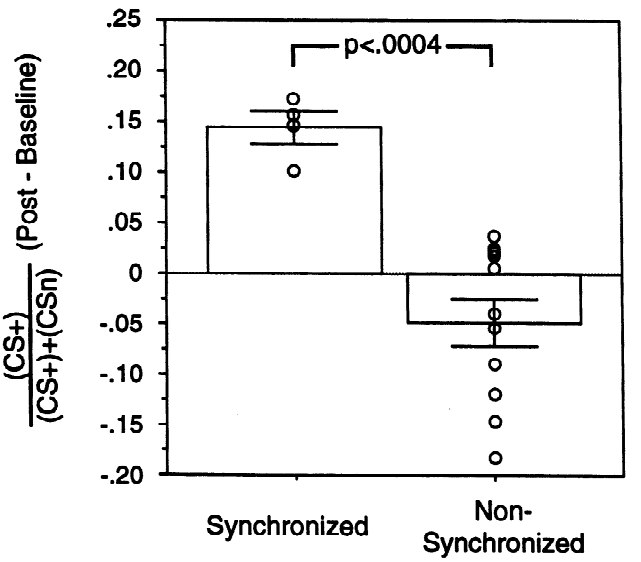

Fig. 8. Greatest increases on plasticity measure were from Synchronized group. The values on the plasticity measure (i.e. the CS+/CSn Index; y-axis) were compared for the Synchronized vs. the Non-synchronized EEG groups (means±S.E.M. for the two groups and individual values for each cell are shown). Notice that there is a significantly higher distribution of values for the Synchronized group. In fact, there was no overlap in values between groups at all; the four highest overall values composed the entire Synchronized group. Considered on its own, this synchronized group underwent a significant increase on the plasticity measure ($P<0.003$, paired t-test, baseline vs. post), whereas the remaining cells, which composed the nonsynchronized group, did not exhibit significant change ($P>0.05$) See text.

the treatment vs. baseline periods. The time window over which firing rates were averaged corresponded to the 200 ms immediately preceding tone onset, which overlapped with the last 150 ms of BasF stimulation. Significant decreases during the treatment were observed for seven cells, while significant increases occurred for only four cells (the four remaining cells showed no significant changes; $P<0.05$, unpaired *t*-tests, treatment vs. baseline), indicating a depressing effect on postsynaptic excitability for the majority of affected cells.

3.7. Control for habituation

It is important to rule out a possible methodological problem that might have reduced the apparent incidence of plasticity. The CS+ tone was repeatedly presented during the treatment period, while the CSn was not. If this repetition caused habituation of responses to the CS+ [20,67], then this might have canceled out or masked the detection of any potentiation induced by the pairing, making it appear that no change had occurred for the CS+.

As indicated in the Materials and methods, the test for habituation involved repeatedly presenting one tone frequency, 240 times at 0.2 Hz, then determining whether or not this caused a specific decrease in ACx response to that frequency (CSr), relative to a control frequency that was not presented during the treatment (the CSn). Results indicated that no cells underwent significant decreases in relative response to the CSr compared with the CSn following the habituation treatment ($P>0.05$, $n=9$, *t*-test). Furthermore, group data indicated no significant changes at any of the post-treatment time-points (Fig. 9). Therefore, habituation can be ruled out.

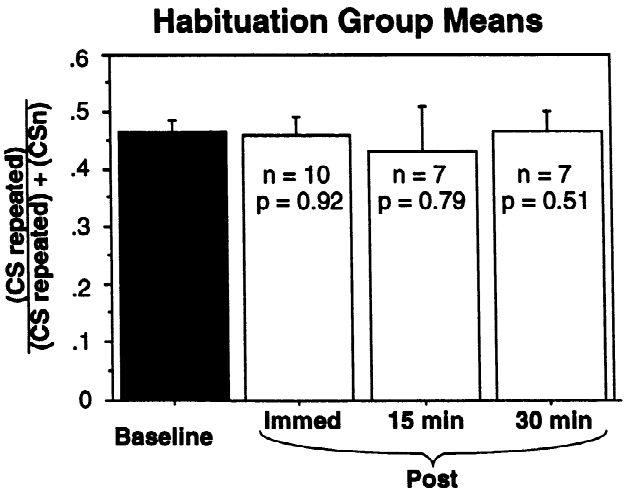

Fig. 9. Habituation experiment: group results. Mean CSr vs. CSn Index values (±S.E.M.) for the baseline and each of the post-'habituation' periods. There are essentially no changes relative to baseline for any of the post-habituation measurements. Probabilities are results of paired *t*-tests (posts vs. baseline, within-cell).

4. Discussion

The combination of BasF stimulation and juxtacellular excitatory current failed to increase CS+ specific responses to tones. In fact, it apparently reduced such plasticity. Lack of plasticity would be expected if the critical hypothesized conditions were not present. However, the failure to observe plasticity does not appear to be due to a failure to control the relevant independent variables in the experiment. For example, during the pairing treatment the excitatory juxtacellular current significantly increased the responses to the CS+ tones for all of the experiments (15/15). Moreover, the BasF stimulation produced non-synchronous cortical EEGs for the majority of the experiments (11/15).

It might be argued the low probability of plasticity was due to habituation to the CS+ tone during the treatment, which might have masked an underlying potentiation. However, no habituation was detected in a control experiment. Thus, overall these results indicate that the conditions hypothesized to be sufficient for plasticity were present.

One might speculate that failure to obtain potentiation could have been due to the relative timing of the presynaptic (tone) input and the postsynaptic (juxtacellular) current. Recent experiments conducted in the neocortex [47] and elsewhere [12,13,45], have indicated that the precise timing of presynaptic and postsynaptic activity can have important consequences for the degree and polarity of plasticity. For example, Markram and colleagues found that in synaptically coupled layer V cells, potentiation occurred when presynaptic input preceded postsynaptic spikes by 10 ms, but depression resulted when postsynaptic spikes preceded presynaptic input by 10 ms [47]. In the present study, the mean response latency to the CS+ during baseline was 27.0±3.5 ms after tone onset, while the average response latency to the compound tone plus current stimulus during the treatment was 15.7±2.9 ms. Thus, on average, spikes were initiated by the juxtacellular postsynaptic stimulus 11.3 ms before the response to the presynaptic tone input. This appears to indicate that the pre/postsynaptic timing in the present experiment is more similar to the situation that produced synaptic depression in the Markram et al. report than that which produced potentiation. However, several other studies of the neocortex have obtained robust potentiation with treatments in which depolarizing postsynaptic stimuli were delivered either before [30,43,54,69] or simultaneous/continuous with the presynaptic input [21,42,69]. In one example, Fregnac et al. [30] found that a synaptic stimulus delivered 5–10 ms after the onset of a depolarizing current pulse, produced synaptic potentiation in 36% of visual cortical

cells and depression in no cells. Similar or stronger effects were reported in the other studies cited above. This evidence suggests that precise pre- vs. postsynaptic timing is unlikely to have been responsible to the failure to observe potentiation in the present study.

4.1. Morphological observations: single cell labeling with biocytin

The biocytin data revealed that the one cell expressing significant potentiation of the relative CS+ response was a layer IV pyramidal cell. This was consistent with the loci of cells expressing plasticity in previous studies of ACx using both BasF pairing and Hebbian protocols [10,23,24]. However, in the present study six other cells were recovered from layer IV, four of them pyramidal, that did not exhibit significant plasticity. The plastic cell had considerably broader upper layer branching than the nonplastic cells, raising the possibility that a larger sample of cells having the laminar and morphological characteristics of the plastic cell might result in a greater incidence of plasticity. The potential importance of upper layer branching might be related to the fact that the density of cholinergic axons in ACx is highest in the upper layers, especially layer I [9,27,46,49]. This implies that cholinergic cells of the BasF would have their strongest influence on cortical neurons with extensive processes in layer I, such as the plastic cell of Fig. 7. While an $n=1$ is too small to permit any conclusions, the correlation of unique upper layers branching with enhanced plasticity suggests that the matter be given further consideration.

4.2. 'Appropriate' conditions were present but may be insufficient or incorrect

The initial discussion indicated that the factors hypothesized to be important for plasticity were present, yet plasticity was not consistently induced. Despite this, it remains possible that the general hypothesis is correct, but that plasticity also requires other factors that were not previously accounted for. The morphological observations above suggest one such potential factor. Another possibility is that the conditions/factors originally hypothesized to be important were not correct. For example, an underlying assumption of the BasF-Covariance hypothesis (see Introduction) is that the BasF stimulation would facilitate Hebbian plasticity by increasing cellular excitability during the pairing treatment. To test for changes in excitability during the treatment, the pre-tone firing rates were compared for the treatment vs. baseline phases of the experiments. There were more decreases than increases in pretone firing rates during the BasF stimulation (seven significant decreases, four significant increases, see Results), supporting the notion that the BasF stimulation reduced, rather than increased, postsynaptic excitability immediately preceding response of the cells to tones. This might have reduced cellular response to tones so that the effectiveness of juxtacellular current on responses to tones was itself reduced.

Unfortunately, the effects of BasF stimulation on the tone/juxtacellular current evoked responses could not be assessed directly because the tone/juxtacellular combination was never presented in the absence of the BasF stimulus. However, it may be possible to estimate these effects indirectly by using results from a previous study that did not involve BasF stimulation [22,24]. These results showed a strong correlation between the numerical sum of the responses to juxtacellular current alone plus responses to tone alone vs. the response to the combined tone/current stimuli (Fig. 10A, $r=0.716$, $P<0.0005$, $n=22$). By applying the regression equation describing this relationship to the results of the present study (and knowing the actual responses to the CS+ alone and juxtacellular current alone in the present study), it was possible to estimate for each cell what the responses to the combined tone/juxtacellular current stimuli would have been had there been no BasF stimuli. Results indicated that for 12/15 cells, the actual responses were weaker than predicted to occur without BasF stimuli (Fig. 10, $P<0.05$, sign test). This finding involves extrapolation from previous studies, so caution should be exercised. However, it does provide some evidence that evoked responses, like tonic excitability (above), were attenuated by the BasF stimuli during the treatment. Thus, although the increase in postsynaptic response during the treatment (produced by the juxtacellular excitatory current) was highly significant, it was not as large as it would have been had there been no BasF stimulus. Further experiments will be required to determine whether or not this apparent attenuation of response during the treatment is strong enough to prevent plastic changes from being induced.

An indication that BasF stimulation may have interfered with plasticity is the finding that the greatest relative potentiation of the CS+ responses occurred during the four experiments in which BasF stimuli were not effective, as assessed by the EEG (Fig. 8). In fact those four experiments, when considered as a group, actually exhibited significant plasticity. In contrast, the 11 experiments in which BasF stimulation was effective at desynchronizing the EEG did not exhibit significant group plasticity. An alternative potential interpretation of these effects is that BasF stimuli for the synchronous group were effective for inducing plasticity but not for EEG desynchronization, whereas the BasF stimuli for the nonsynchronous group were more effective on the EEG and less effective (possibly too strong) for plasticity. A parametric study, examining different intensities and durations of BasF stimulation, might help to resolve this issue. In summary, it is possible that the BasF stimulation in the present experiment disrupted Hebbian plasticity, perhaps by decreasing cellular excitability.

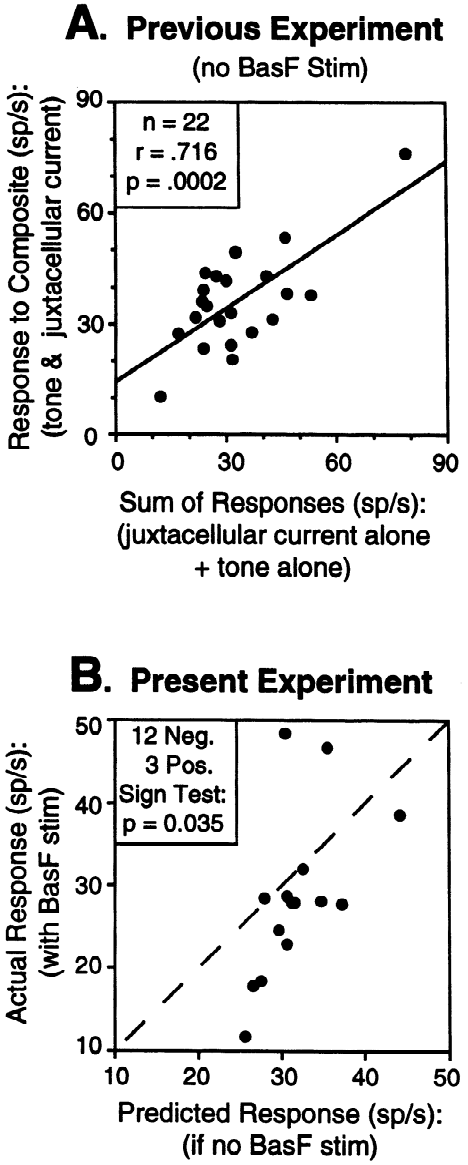

Fig. 10. Calculated effect of BasF stimulation on tone-evoked responses. (A) Regression plot from previous experiment [22] illustrating relationship between sum of individual responses to tone and positive juxtacellular current (*x*-axis) vs. actual response to tone/current composite stimulus (*y*-axis). Note the strong positive correlation. The regression equation describing this relationship is $0.66(x) + 14.4 = y$, and can be thought of as a way to predict the response to the composite, given the sum of the responses to the individual stimuli. Note that the experiment from which the regression equation was derived involved no BasF stimulation [22]. (B) Predicted vs. actual responses during treatment for present experiment. The *x*-axis is the predicted response to the tone/current composite stimulus if there had been no BasF stimulus. Values for this axis were calculated by summing the individual responses to the tone and juxtacellular current stimuli for the present experiment, then entering these sums into the regression equation obtained in A. The *y*-axis represents the actual response to the tone/current composite, in the presence of BasF stimulation. Points falling above the diagonal dashed line indicate that the actual response is higher than the predicted response. Points falling below the diagonal indicate the actual response is lower than predicted. Notice that 12/15 points fall below the line. Because the actual responses in the presence of BasF stimulation are significantly lower than the responses predicted to occur in the absence of BasF stimulation, it would appear that the BasF stimulation had a depressing effect on evoked response.

4.3. Simple 'BasF-covariance hypothesis' may be incorrect

Neither depression of excitability nor disruption of plasticity were predicted outcomes of BasF stimulation. Cortical excitability is generally thought to be increased during manipulations/states associated with high BasF activity (e.g., direct BasF stimulation, behavioral arousal/cortical desynchrony, cortical perfusion of ACh; reviewed in Sillito [61] and Cruikshank and Weinberger [23]. The present results indicate that this may be an oversimplification. This conclusion is supported by recent studies of BasF function in ACx. For example, a number of in vitro studies in the ACx have indicated that the effects of acetylcholine, which is normally released from cholinergic fibers of the BasF in vivo, can be quite complicated. Excitatory synaptic potentials can be either increased or decreased by ACh depending on a number of circumstances including initial strength of response, the presence/absence of preceding stimuli, and the degree of inhibition [7,8,52].

These complications are echoed by anatomical findings. For example, it has been reported that cholinergic fibers of the BasF synapse not only on pyramidal cells, but also on inhibitory cells of the neocortex [6,11,37], and reviewed in Mesulam [49]. Thus, these inhibitory cells may be excited by BasF stimuli and, in turn, inhibit pyramidal cells (which made up the majority of the cells recorded in the present study). There are also direct inhibitory projections (i.e. containing GABA) from the BasF to the neocortex. Although the majority of these projections may synapse on neocortical GABAergic cells, producing disinhibition of pyramidal cells [26], there are inhibitory projections from the BasF to cortical targets that are negative for GABA [33]. Such projections may explain the observation that BasF stimulation can produce inhibition of cortical unit activity [39].

The present experiments were partly motivated by an earlier study in which auditory cortical plasticity was induced using a modified Hebbian treatment, without any BasF stimulation [24]. In that study, at two-tone discrimination paradigm was applied, in which a CS+ tone was paired with excitatory postsynaptic current and a CS− tone was paired with inhibitory postsynaptic current. The protocol produced enduring changes in response favoring the CS+ relative to the CS−, and was most effective when the cortical EEG was desynchronized during the pairing treatment. It was hypothesized that the facilitated plasticity occurring during EEG desynchrony might be mediated by cholinergic excitation of the postsynaptic cells during the CS+ portion of the pairing treatment [22]. Therefore in the present experiment, the cholinergic BasF was stimulated during CS+ Hebbian pairing, and no CS− pairings were administered. The failure of the present protocol to induce potentiation of CS+ responses encourages reconsideration of the original hypothesis. For exam-

ple, it is possible that the CS− pairings in the previous discrimination experiment may have played a more important role than originally thought (e.g., [30]), and the facilitation of plasticity by cortical desynchronization may have been mediated through effects on the CS−, rather than completely via the CS+. The combined effects of BasF stimulation in the present experiment (i.e. EEG desynchronization 'and' suppression of cellular excitability) are consistent with the latter possibility. This issue calls for further investigation.

5. Conclusions

The present findings may be seen as negative insofar as BasF stimulation immediately preceding cellular excitation to tone/juxtacellular current failed to increase frequency-specific plasticity of responses to tone. However, this outcome appears to have uncovered additional considerations in the potential relationships between BasF and Hebbian/covariance processes. Specifically, BasF stimulation actually decreased background excitability of cortical cells in the majority of cases and greater Hebbian/covariance plasticity occurred in the absence of BasF-induced changes in the EEG. The present observations are compatible with two explanations: either the BasF-Hebbian covariance hypothesis is wrong or plasticity in this situation requires factors other than those indexed by BasF-induced EEG desynchronization or current-induced facilitation of cellular responses to tones (e.g., the morphological cell type, above). This study does not permit a choice between the two possibilities.

Acknowledgements

Supported by NIH-NIDCD research grants #DC 02938 and #DC02346 (N.M.W.) and MH10432-03 (S.C.).

References

[1] E. Ahissar, M. Ahissar, Plasticity in auditory cortical circuitry, Curr. Opin. Neurobiol. 4 (1994) 500–507.
[2] E. Ahissar, M. Abeles, M. Ahissar, S. Haidarliu, E. Vaadia, Hebbian-like functional plasticity in the auditory cortex of the behaving monkey, Neuropharmacology 37 (1998) 633–655.
[3] E. Ahissar, S. Haidarliu, D.E. Shulz, Possible involvement of neuromodulatory systems in cortical Hebbian-like plasticity, J. Physiol. Paris 90 (1996) 353–360.
[4] E. Ahissar, E. Vaadia, M. Ahissar, H. Bergman, A. Arieli, M. Abeles, Dependence of cortical plasticity on correlated activity of single neurons and on behavioral context, Science 257 (1992) 1412–1415.
[5] R.D. Andrew, M. Fagan, A technique for controlling the membrane potential of neurons during unit recording, J. Neurosci. Methods 33 (1990) 55–60.
[6] C. Aoki, S. Kabak, Cholinergic terminals in the cat visual cortex: ultrastructural basis for interaction with glutamate-immunoreactive neurons and other cells, Vis. Neurosci. 8 (1992) 177–191.
[7] V.B. Aramakis, A.E. Bandrowski, J.H. Ashe, Activation of muscarinic receptors modulates NMDA receptor-mediated responses in auditory cortex, Exp. Brain Res. 113 (1997) 484–496.
[8] V.B. Aramakis, A.E. Bandrowski, J.H. Ashe, Muscarinic reduction of GABAergic synaptic potentials results in disinhibition of the AMPA/kainate-mediated EPSP in auditory cortex, Brain Res. 758 (1997) 107–117.
[9] C. Avendano, D. Umbriaco, R.W. Dykes, L. Descarries, Acetylcholine innervation of sensory and motor neocortical areas in adult cat: a choline acetyltransferase immunohistochemical study, J. Chem. Neuroanat. 11 (1996) 113–130.
[10] J.S. Bakin, N.M. Weinberger, Induction of a physiological memory in the cerebral cortex by stimulation of the nucleus basalis [see comments], Proc. Natl. Acad. Sci. USA 93 (1996) 11219–11224.
[11] C. Beaulieu, P. Somogyi, Enrichment of cholinergic synaptic terminals on GABAergic neurons and coexistence of immunoreactive GABA and choline acetyltransferase in the same synaptic terminals in the striate cortex of the cat, J. Comp. Neurol. 304 (1991) 666–680.
[12] C. C Bell, V.Z. Han, Y. Sugawara, K. Grant, Synaptic plasticity in a cerebellum-like structure depends on temporal order, Nature 387 (1997) 278–281.
[13] G.Q. Bi, M.M. Poo, Synaptic modifications in cultured hippocampal neurons: dependence on spike timing, synaptic strength, and postsynaptic cell type, J. Neurosci. 18 (1998) 10464–10472.
[14] E. Bienenstock, Y. Fregnac, S. Thorpe, Ionophoretic clamp of activity in visual cortical neurons in the cat: a test of Hebb's hypothesis, J. Physiol. (Lond.) 345 (1983) 123P.
[15] T.S. Bjordahl, M.A. Dimyan, N.M. Weinberger, Induction of long-term receptive field plasticity in the auditory cortex of the waking guinea pig by stimulation of the nucleus basalis, Behav. Neurosci. 112 (1998) 467–479.
[16] J.F. Brons, C.D. Woody, N. Allon, Changes in excitability to weak-intensity extracellular electrical stimulation of units of pericruciate cortex in cats, J. Neurophysiol. 47 (1982) 377–388.
[17] J. Buchhalter, J. Brons, C.D. Woody, Changes in cortical neuronal excitability after presentations of a compound auditory stimulus, Brain Res. 156 (1978) 162–167.
[18] D.V. Buonomano, Distinct functional types of associative long-term potentiation in neocortical and hippocampal pyramidal neurons, J. Neurosci. 19 (1999) 6748–6754.
[19] F. Casamenti, G. Deffenu, A.L. Abbamondi, G. Pepeu, Changes in cortical acetylcholine output induced by modulation of the nucleus basalis, Brain Res. Bull. 16 (1986) 689–695.
[20] C. Condon, N.M. Weinberger, Habituation produces frequency-specific plasticity of receptive fields in auditory cortex, Behav. Neurosci. 105 (1991) 416–430.
[21] M.C. Crair, R.C. Malenka, A critical period for long-term potentiation at thalamocortical synapses [see comments], Nature 375 (1995) 325–328.
[22] S.J. Cruikshank, Evaluation of the Hebbian covariance hypothesis in receptive field plasticity of adult auditory cortical neurons, Thesis (Ph.D., Biological Sciences) — University of California, Irvine, (1997).
[23] S.J. Cruikshank, N.M. Weinberger, Evidence for the Hebbian hypothesis in experience-dependent physiological plasticity of neocortex: a critical review, Brain Res. Rev. 22 (1996) 191–228.
[24] S.J. Cruikshank, N.M. Weinberger, Receptive-field plasticity in adult auditory cortex induced by Hebbian covariance, J. Neurosci. 16 (1996) 861–875.
[25] M.A. Dimyan, N.M. Weinberger, Basal forebrain stimulation induces discriminative receptive field plasticity in auditory cortex, Behav. Neurosci. 113 (1999) 691–702.
[26] R.W. Dykes, Mechanisms controlling neuronal plasticity in somatosensory cortex, Can. J. Physiol. Pharmacol. 75 (1997) 535–545.

[27] F.P. Eckenstein, R.W. Baughman, J. Quinn, An anatomical study of cholinergic innervation in rat cerebral cortex, Neuroscience 25 (1988) 457–474.
[28] J.-M. Edeline, B. Hars, C. Maho, E. Hennevin, Transient and prolonged facilitation of tone-evoked responses induced by basal forebrain stimulations in the rat auditory cortex, Exp. Brain Res. 97 (1994) 373–386.
[30] Y. Fregnac, J.P. Burke, D. Smith, M.J. Friedlander, Temporal covariance of pre- and postsynaptic activity regulates functional connectivity in the visual cortex, J. Neurophysiol. 71 (1994) 1403–1421.
[31] Y. Fregnac, D. Shulz, Models of synaptic plasticity and cellular analogs of learning in the developing and adult vertebrate visual cortex, in: V. Casagrande, P. Shinkman (Eds.), Advances in Neural and Behavioral Development, Vol. 4, Ablex Publ. Corp, New Jersey, 1994, pp. 149–252.
[32] Y. Fregnac, D. Shulz, S. Thorpe, E. Bienenstock, A cellular analogue of visual cortical plasticity, Nature 333 (1988) 367–370.
[33] T.F. Freund, A.I. Gulyas, GABAergic interneurons containing calbindin D28K or somatostatin are major targets of GABAergic basal forebrain afferents in the rat neocortex, J. Comp. Neurol. 314 (1991) 187–199.
[34] B. Hars, C. Maho, J.-M. Edeline, E. Hennevin, Basal forebrain stimulation facilitates tone-evoked responses in the auditory cortex of awake rat, Neuroscience 56 (1993) 61–74.
[35] D.O. Hebb, Organization of Behavior, Wiley, New York, 1949.
[36] K. Horikawa, W.E. Armstrong, A versatile means of intracellular labeling: injection of biocytin and its detection with avidin conjugates, J. Neurosci. Methods 25 (1988) 1–11.
[37] C.R. Houser, G.D. Crawford, P.M. Salvaterra, J.E. Vaughn, Immunocytochemical localization of choline acetyltransferase in rat cerebral cortex: a study of cholinergic neurons and synapses, J. Comp. Neurol. 234 (1985) 17–34.
[38] J.I. Hubbard, R. Llinas, D.M. Quastel, Electrophysiological Analysis of Synaptic Transmission, Edward Arnold, London, 1969.
[39] M.E. Jimenez-Capdeville, R.W. Dykes, A.A. Myasnikov, Differential control of cortical activity by the basal forebrain in rats: a role for both cholinergic and inhibitory influence, J. Comp. Neurol. 381 (1997) 53–67.
[40] S.L. Juliano, Mapping the sensory mosaic [comment], Science 279 (1998) 1653–1654.
[41] M.P. Kilgard, M.M. Merzenich, Cortical map reorganization enabled by nucleus basalis activity [see comments], Science 279 (1998) 1714–1718.
[42] A. Kirkwood, M.F. Bear, Hebbian synapses in visual cortex, J. Neurosci. 14 (1994) 1634–1645.
[43] A. Kossel, T. Bonhoeffer, J. Bolz, Non-Hebbian synapses in rat visual cortex, NeuroReport 1 (1990) 115–118.
[44] M. Kurosawa, A. Sato, Y. Sato, Stimulation of the nucleus basalis of Meynert increases acetylcholine release in the cerebral cortex of the rat, Neurosci. Lett. 98 (1989) 45–50.
[45] D.J. Linden, The return of the spike: postsynaptic action potentials and the induction of LTP and LTD, Neuron 22 (1999) 661–666.
[46] A. Lysakowski, B.H. Wainer, G. Bruce, L.B. Hersh, An atlas of the regional and laminar distribution of choline acetyltransferase immunoreactivity in rat cerebral cortex, Neuroscience 28 (1989) 291–336.
[47] H. Markram, J. Lubke, M. Frotscher, B. Skmann, Regulation of synaptic efficacy by coincidence of postsynaptic APs and EPSPs [see comments], Science 275 (1997) 213–215.
[48] D.A. McCormick, Neurotransmitter actions in the thalamus and cerebral cortex, J. Clin. Neurophysiol. 9 (1992) 212–223.
[49] M.M. Mesulam, The systems-level organization of cholinergic innervation in the human cerebral cortex and its alterations in Alzheimer's disease, Prog. Brain Res. 109 (1996) 285–297.
[50] R. Metherate, J.H. Ashe, Basal forebrain stimulation modifies auditory cortex responsiveness by an action at muscarinic receptors, Brain Res. 559 (1991) 163–167.
[51] R. Metherate, J.H. Ashe, Nucleus basalis stimulation facilitates thalamocortical synaptic transmission in the rat auditory cortex, Synapse 14 (1993) 132–143.
[52] R. Metherate, J.H. Ashe, Synaptic interactions involving acetylcholine, glutamate, and GABA in rat auditory cortex, Exp. Brain Res. 107 (1995) 59–72.
[53] R. Metherate, C.L. Cox, J.H. Ashe, Cellular bases of neocortical activation: modulation of neuronal oscillations by the nucleus basalis and endogenous acetylcholine, J. Neurosci. 12 (1992) 4701–4711.
[54] Y. Otsu, F. Kimura, T. Tsumoto, Hebbian induction of LTP in visual cortex: perforated patch-clamp study in cultured neurons, J. Neurophysiol. 74 (1995) 2437–2444.
[55] G. Paxinos, C. Watson, The Rat Brain in Stereotaxic Coordinates, Academic Press, New York, 1982.
[56] A. Peters, E.G. Jones, Cerebral Cortex, Vol. 1, Plenum Press, New York, 1984.
[57] D. Pinault, Golgi-like labeling of a single neuron recorded extracellularly, Neurosci. Lett. 170 (1994) 255–260.
[58] D. Pinault, A novel single-cell staining procedure performed in vivo under electrophysiological control: morpho-functional features of juxtacellularly labeled thalamic cells and other central neurons with biocytin or Neurobiotin, J. Neurosci. Methods 65 (1996) 113–136.
[59] R. Schliebs, S. Rossner, V. Bigl, Immunolesion by 192IgG-saporin of rat basal forebrain cholinergic system: a useful tool to produce cortical cholinergic dysfunction, Prog. Brain Res. 109 (1996) 253–264.
[60] T.J. Sejnowski, G. Tesauro, The Hebb rule for synaptic plasticity: algorithms and implementations, in: J.H. Byrne, W.O. Berry (Eds.), Neural Models of Plasticity, Academic Press, San Diego, 1989, pp. 94–101.
[61] A.M. Sillito, The cholinergic neuromodulatory system: an evaluation of its functional roles, Prog. Brain Res. 98 (1993) 371–378.
[62] G.S. Stent, A physiological mechanism for Hebb's postulate of learning, Proc. Natl. Acad. Sci. USA 70 (1973) 997–1001.
[63] M. Steriade, D.A. McCormick, T.J. Sejnowski, Thalamocortical oscillations in the sleeping and aroused brain, Science 262 (1993) 679–685.
[64] F. Strumwasser, S. Rosenthal, Prolonged and patterned direct extracellular stimulation of single neurons, Am. J. Physiol. 198 (1960) 405–413.
[65] N. Suga, T. Manabe, Neural basis of amplitude-spectrum representation in auditory cortex of the mustached bat, J. Neurophysiol. 47 (1982) 225–255.
[66] N.M. Weinberger, Tuning the brain by learning and by stimulation of the nucleus basalis, Trends Cogn. Sci. 2 (1998) 271–273.
[67] N.M. Weinberger, T.D. Oleson, J.H. Ashe, Sensory system neural activity during habituation of the pupillary orienting reflex, Behav. Biol. 15 (1975) 283–301.
[68] C.D. Woody, J.D. Knispel, T.J. Crow, P.A. Black-Cleworth, Activity and excitability to electrical current of cortical auditory receptive neurons of awake cats as affected by stimulus association, J. Neurophysiol. 39 (1976) 1045–1061.
[69] Y. Yoshimura, T. Tsumoto, Dependence of LTP induction on postsynaptic depolarization: a perforated patch-clamp study in visual cortical slices of young rats, J. Neurophysiol. 71 (1994) 1638–1645.